HEALTH AND MEDICINE

Data for all: Tactile graphics that light up with picture-perfect resolution

Jordan C. Koone[1]†, Chad M. Dashnaw[1]†, Emily A. Alonzo[1], Miguel A. Iglesias[1], Kelly-Shaye Patero[1], Juan J. Lopez[1], Ao Yun Zhang[1], Bernd Zechmann[2], Noah E. Cook[1], Mona S. Minkara[3], Cary A. Supalo[4], Hoby B. Wedler[5], Matthew J. Guberman-Pfeffer[6], Bryan F. Shaw[1]*

People who are blind do not have access to graphical data and imagery produced by science. This exclusion complicates learning and data sharing between sighted and blind persons. Because blind people use tactile senses to visualize data (and sighted people use eyesight), a single data format that can be easily visualized by both is needed. Here, we report that graphical data can be three-dimensionally printed into tactile graphics that glow with video-like resolution via the lithophane effect. Lithophane forms of gel electropherograms, micrographs, electronic and mass spectra, and textbook illustrations could be interpreted by touch or eyesight at ≥79% accuracy (n = 360). The lithophane data format enables universal visualization of data by people regardless of their level of eyesight.

INTRODUCTION

Science educators, researchers, publishers, and policymakers continue to overlook the need to make the graphical data and imagery of science accessible to persons who are blind or have low vision (*1*–*4*). This inaccessibility pairs poorly with aspirations of diversability (*5*–*10*). In rare cases when data are made accessible with tactile graphics, physical models, audio, or Braille, the formats may be of low resolution or quality and not amenable to sharing with sighted individuals (*11*–*13*). There is a need for a high-resolution data format that can be visualized by anyone regardless of eyesight. Such a format will enable blind and sighted individuals to share—to visualize and discuss—the exact same piece of data. This format must be intuitive, inexpensive, portable, and storable in a research notebook.

We hypothesized that the lithophane—an old-fashioned art form (*14*)—might function as a universally visualizable data format, interpretable by tactile sensing or eyesight. A lithophane is a thin, translucent engraving, typically <2 mm in thickness (Fig. 1). The surface appears opaque in ambient light or "front" light (Fig. 1A). However, the lithophane glows like a digital image when held in front of any light source (e.g., back lit by a ceiling light in Fig. 1B and sunlight in Fig. 1C). The scattering of light through the translucent material causes thinner regions to appear brighter and thicker regions to appear darker. The use of lithophanes as a universally visualized data format has never been reported.

Historically, lithophanes were made from thin porcelain or wax (*14*) beginning in 17th-century Europe but possibly a millennium earlier in China (*15*). Lithophanes, including those made in this study, can now be three-dimensionally (3D) printed from any 2D image after the image is converted to a 3D topograph with free online software (*16*).

In this study, we focused on creating and testing lithophanes of data found in the chemical sciences. The exclusion of students with blindness from chemistry is explicit (fig. S1) and systematic (*12*, *17*, *18*). This exclusion can be viewed as a virtue by educators, parents, peers, or self, on the basis of laboratory safety and the "visual" nature of chemistry (*17*). However, exclusion from chemistry impedes learning in other fields that might be more inclusive. Four authors of the current paper have been blind since birth or childhood and are among the few persons that earned PhD degrees in the chemical sciences while being blind (*8*, *11*, *12*, *18*).

RESULTS AND DISCUSSION

This study was approved by the Institutional Review Board at Baylor University. Lithophanes were created using a small commercial 3D printer, costing <$5000 (a Form 3B+ printer from formlabs). We compared how blind (or blindfolded) and sighted people interpreted lithophane data by tactile sensing or eyesight. Participants included blind PhD chemists and students, and sighted students with or

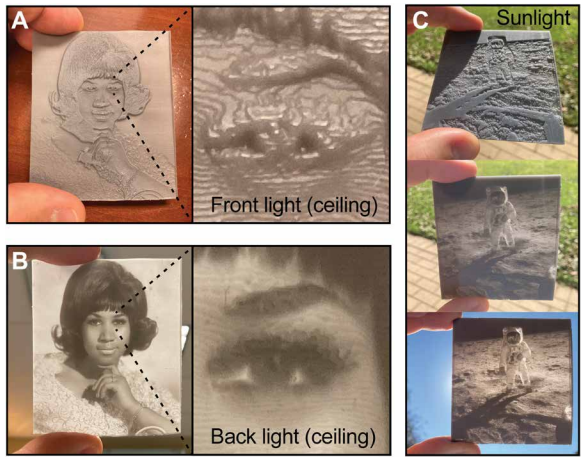

Fig. 1. Three-dimensionally printed lithophanes of popular imagery. (**A**) Appearance of lithophane with front lighting (from overhead ceiling lights). (**B**) Same lithophane in (A) held up to the same ceiling light for back lighting. (**C**) Lithophane illuminated with natural outdoor lighting (front and back). Image credit: NASA. These images are in the public domain in the United States (i.e., published between 1926 and 1977 without a copyright notice).

[1]Department of Chemistry and Biochemistry, Baylor University, Waco, TX, USA. [2]Center for Microscopy and Imaging, Baylor University, Waco, TX, USA. [3]Department of Bioengineering, Northeastern University, Boston, MA, USA. [4]Educational Testing Services, Princeton, NJ, USA. [5]Wedland Group, Petaluma, CA, USA. [6]Department of Molecular Biophysics and Biochemistry, Yale University, New Haven, CT, USA.
*Corresponding author. Email: bryan_shaw@baylor.edu
†These authors contributed equally to this work.

without blindfolds. We initially focused on the most common data type in biochemistry: SDS–polyacrylamide gel electrophoresis (SDS-PAGE; Figs. 2 and 3). Making the data of gel electrophoresis accessible to persons with blindness will increase their access to the life sciences (*19*).

Lithophane forms of four other data types were also fabricated, including scanning electron microscopy (SEM) of a butterfly chitin scale (Fig. 4), a mass spectrum of a protein with gas phase phosphate adducts (Fig. 5), and an electronic [ultraviolet-visible (UV-vis)] spectrum of an iron-porphyrin protein (Fig. 6). We also prepared a textbook style secondary structure map of a seven-stranded β sheet protein (with two Greek-key loops) (Fig. 7). The five lithophanes were fabricated to a size of approximately 70 mm by 60 mm by 0.5 mm (about the size of an identification card). The printing of larger lithophanes (e.g., 210 mm by 150 mm) could accommodate more complex data at a greater magnification.

Each lithophane perfectly matched the digital image from which it was created, down to the finest details (Figs. 2 and 4 to 7). With SDS-PAGE, the darkness of each band in the digital image is proportional to the protein concentration (Fig. 2, C and D). This correlation is preserved in the lithophane, according to densitometric integration of bands in the digital images of the gel and the back-lit lithophane (Fig. 2, C and D). The height of the bands in the SDS-PAGE lithophane (which determines the darkness of the band when back lit) correlates to the darkness of the band in the digital image of the gel [R^2 = 0.9747 for carbonic anhydrase (CA) and R^2 = 0.9674 for superoxide dismutase 1 (SOD1); Fig. 2D]. In the lithophane of the butterfly scale, the individual chitin fibrils are well resolved and separated at a distance of 0.4 mm (Fig. 4B). In the case of the mass spectrum, the level of noise in the spectrum (corresponding to a signal-to-noise ratio of 4.6) was projected sharply by the lithophane (Fig. 5B).

The ability to interpret each of the five lithophanes by tactile sensing was tested on a cohort of 106 sighted persons with blindfolds and 5 persons who are blind. These blind persons (four of which have earned PhD degrees in chemistry) are coauthors of this study but did not participate in the design of the specific datasets. A separate cohort of sighted participants who were not blindfolded (n = 106) was asked to interpret back-lit lithophanes using eyesight. Because lithophanes are intended to be back lit with indoor room lighting (ambient light), test participants were instructed to backlight lithophanes by holding the lithophane up to the overhead classroom lights. The overhead room lights were standard 28-W fluorescent light bulbs. To compare the clarity of the lithophane with the master image, a third group of sighted persons were asked to use eyesight to interpret the original digital image as it appeared on a computer screen (n = 143).

The details of each test, including test questions, answers, and raw data, can be found in the Supplementary Materials (fig. S2 and data S1 and S2). During all tests (visual or tactile), all alphanumeric information such as axis values or scale bars was read continuously from a Word document using the text-to-speech function. This

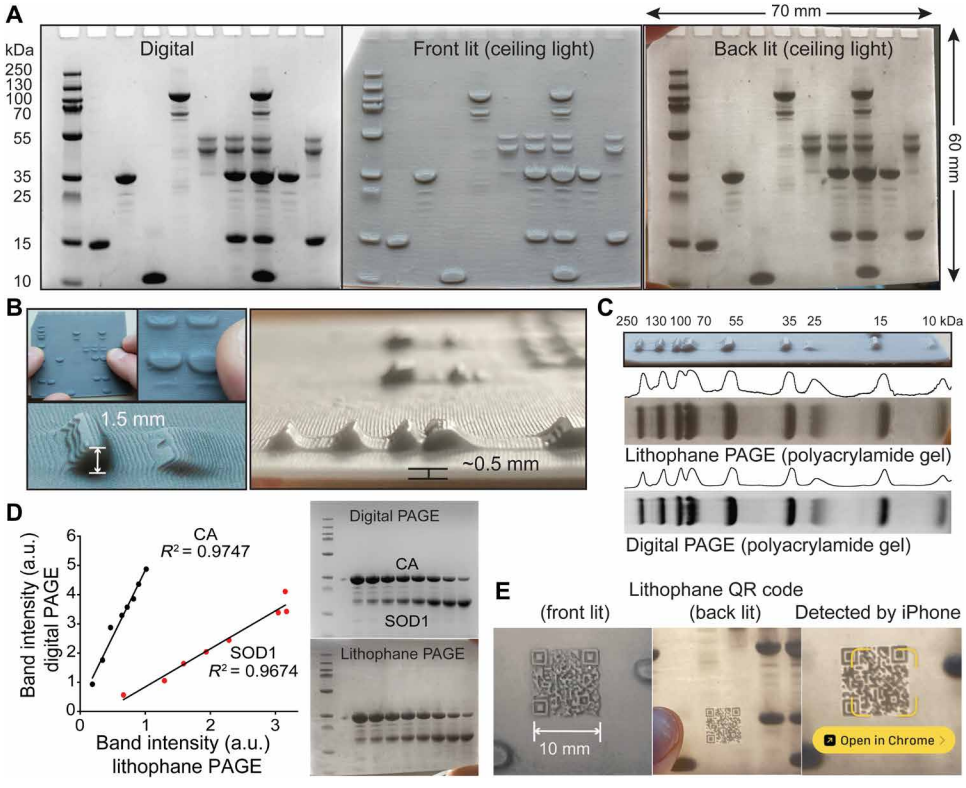

Fig. 2. SDS-PAGE dataset in LDF. (**A**) Conversion of an SDS-PAGE into the lithophane format used for testing. From left to right: Digital source image of SDS-PAGE, front-lit SDS-PAGE lithophane, and back-lit SDS-PAGE lithophane. (**B**) Magnification of raised bands in SDS-PAGE (LDF, lithophane data format). (**C**) Comparison of signal intensity in marker lane of back-lit lithophane (top) and actual polyacrylamide gel (bottom). Integration of band darkness is shown for each set. Front-lit lithophane is shown for reference, with molecular weights indicated. (**D**) Integration of band intensity in dilution series of proteins from digital image of SDS-PAGE and back-lit lithophane (CA, carbonic anhydrase; SOD1, superoxide dismutase 1). a.u. arbitrary units. (**E**) A 3D-printed lithophane quick response (QR) code (10 mm) can link to audio or text details of data.

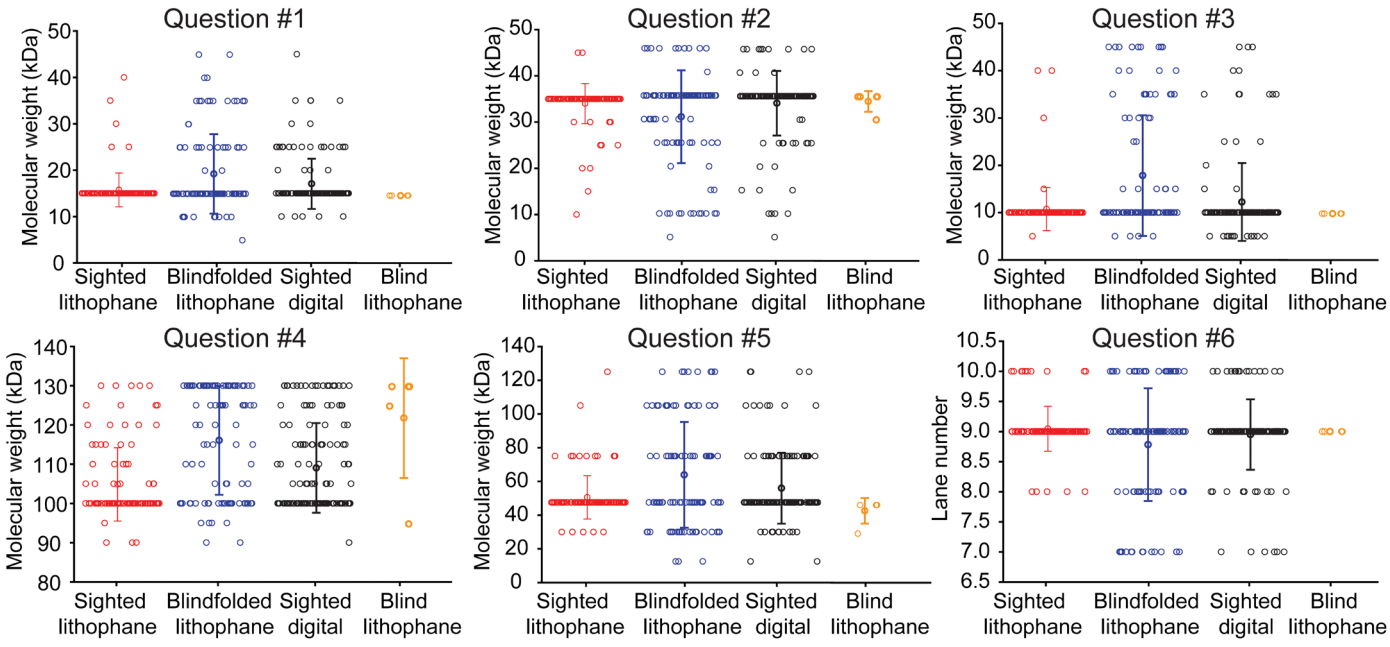

Fig. 3. Distribution of answers provided by 360 participants for each question of the SDS-PAGE lithophane. Error bars represent the SD of the mean. The quantitative answers to each question can be found in Table 1. The actual questions can be found in Materials and Methods.

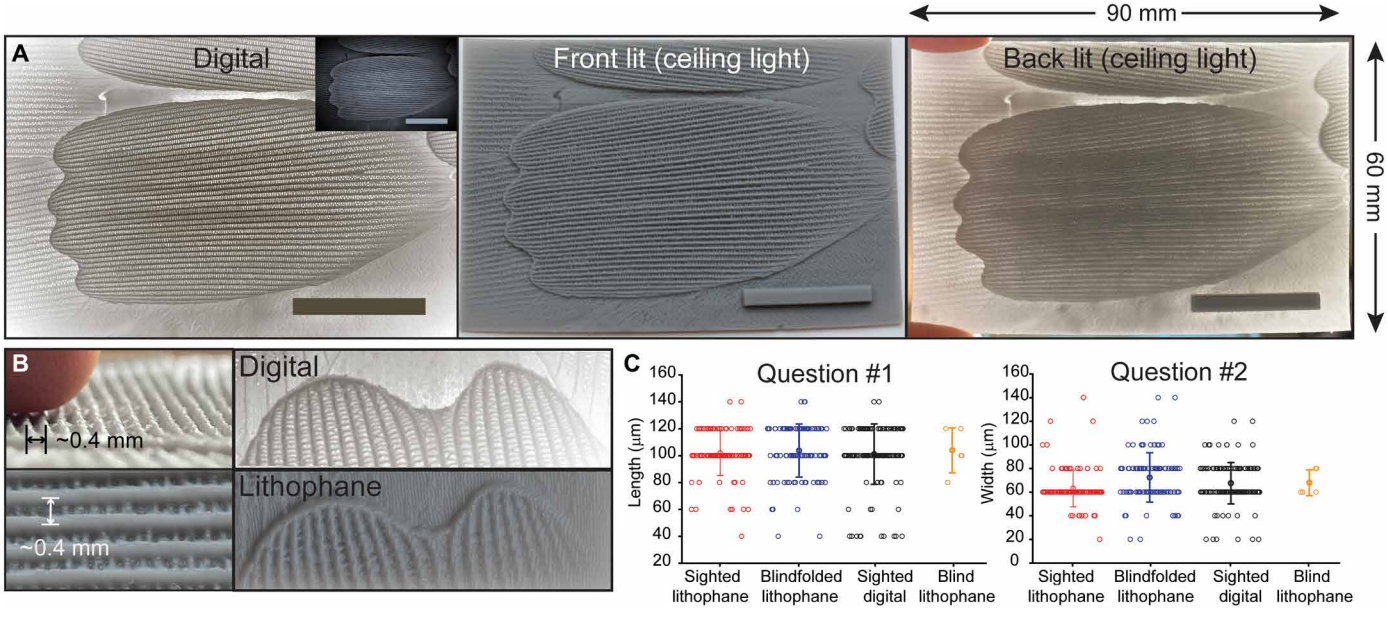

Fig. 4. Scanning electron micrograph of the butterfly scale in LDF. (**A**) Conversion of an SEM into the lithophane format used for testing. From left to right: Digital source image of the SEM, front-lit SEM lithophane, and back-lit SEM lithophane. The length of the scale bar in the lower right-hand corner represents 40 μm. (**B**) Magnification of butterfly scales in the scanning electron micrograph. Individual chitin fibrils were accurately fabricated by the 3D printer, at a spacing of 0.4 mm in the final lithophane. (**C**) Distribution of answers provided by 360 participants for each question regarding the SEM lithophane.

information can also be encoded into the lithophane as a 3D quick response (QR) code (Fig. 2E). Braille was not used in this study because less than 10% of blind persons are Braille readers (*20*).

For tactile and visual tests of SDS-PAGE lithophanes and digital images, participants were asked to use the molecular mass marker in lane 1 to determine (i) the mass of the most abundant bands in lanes 2 to 6 (left to right) and (ii) integrate signals to discern which lane, of lanes 7 to 10, was most pure. For mass spectra and UV-vis spectra, participants were asked to approximate the mass of peaks or the wavelength of the peaks (as well as the value of absorbance). For SEM, participants were asked to approximate the dimensions of the single chitin scale. For protein topology, participants were asked

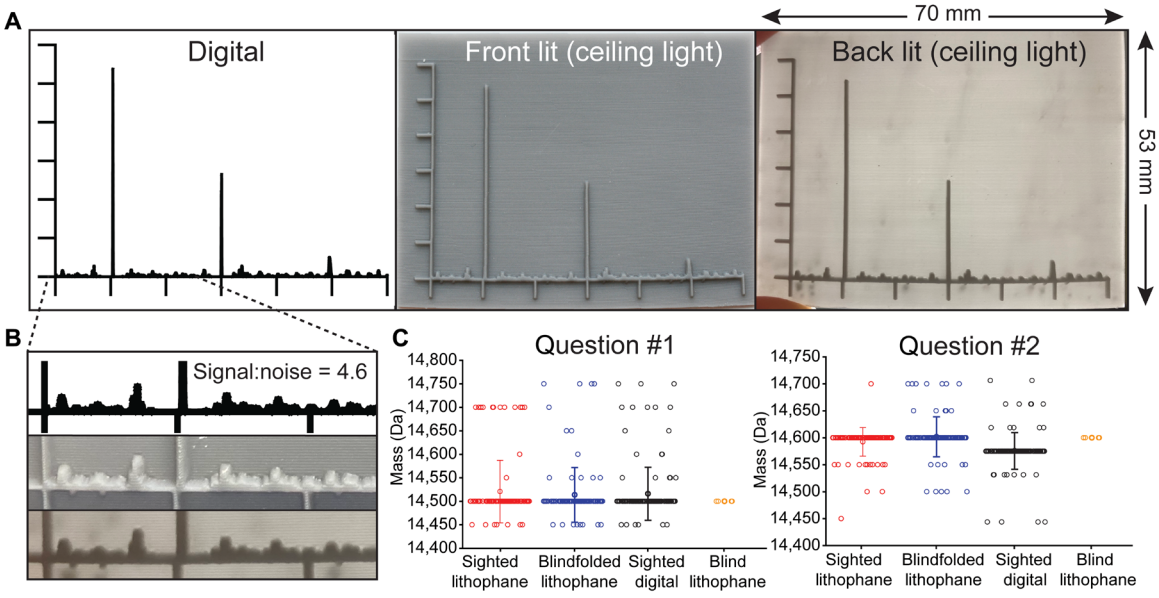

Fig. 5. Mass spectrum of a protein molecule in LDF. (**A**) Conversion of a mass spectrum into the lithophane format used for testing. From left to right: Digital source image of the mass spectrum, front-lit mass spectrum lithophane, and back-lit mass spectrum lithophane. (**B**) Magnification of noise in digital image and lithophane formats (front and back lighting). (**C**) Distribution of answers provided by 360 participants for each question regarding the mass spectrum lithophane.

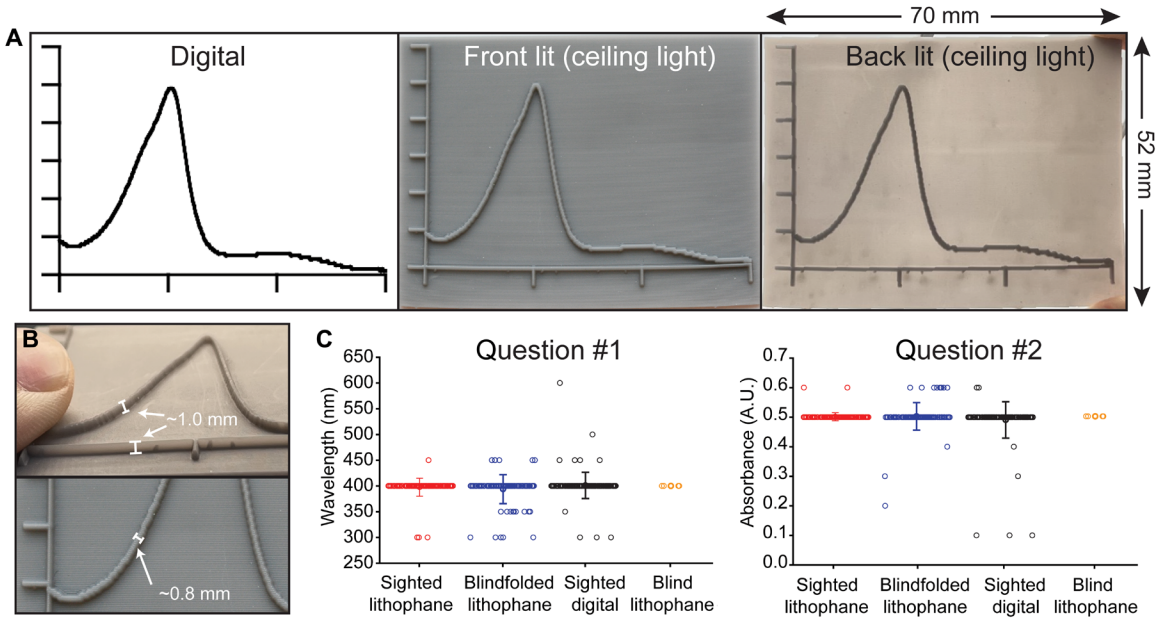

Fig. 6. UV-vis spectrum of heme protein in LDF. (**A**) Conversion of a UV-vis spectrum into the lithophane format used for testing. From left to right: Digital source image of the UV-vis spectrum, front-lit UV-vis spectrum lithophane, and back-lit UV-vis spectrum lithophane. (**B**) The tactile features of the lithophane UV-vis spectrum, including the *x*/*y* axis and spectral curve, are 0.8 and 1.0 mm in width and height, respectively. (**C**) Distribution of answers provided by 360 participants for each question regarding the UV-vis spectrum lithophane.

how many β strands were present and whether the strands were predominantly parallel (↑↑) or antiparallel (↓↑).

In general, participants who were blind or blindfolded used tactile sensing to accurately interpret all five lithophanes. Sighted participants viewed back-lit lithophanes using only eyesight. A summary of the accuracy of data interpretation by tactile sensing and eyesight (back-lit lithophane or digital image) can be found in Table 1. The distribution of raw answers for each question, asked of each dataset, is shown in Fig. 3 (for SDS-PAGE) and in Figs. 4C, 5C, 6C, and 7C [for SEM, mass spectrometry (MS), UV-vis spectroscopy, and protein topology].

The interpretation of some data is subjective with correct answers spanning a range of values. For example, the molecular weights of migrating bands at higher molecular weight in SDS-PAGE (>70 kDa)

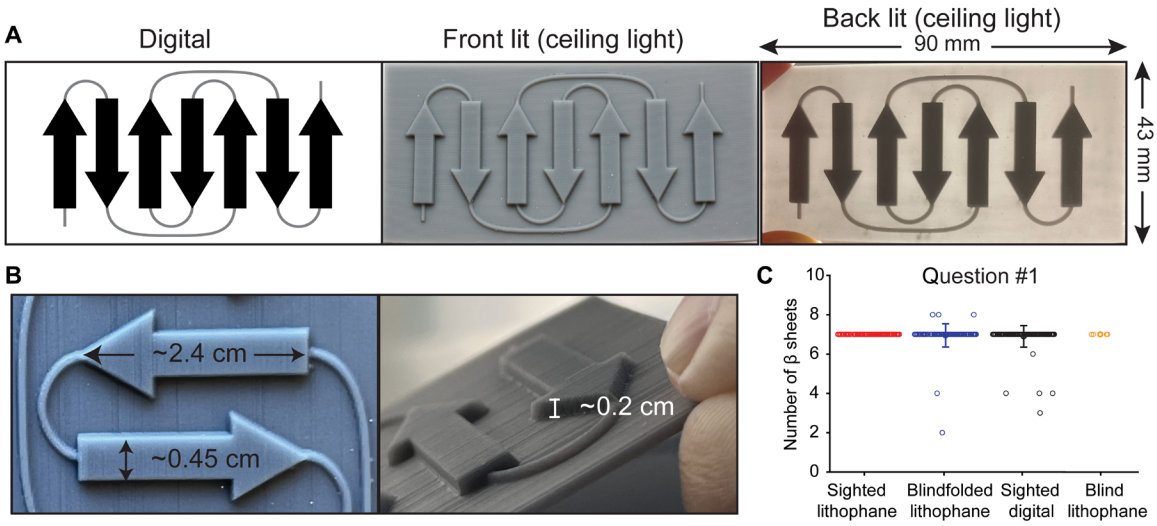

Fig. 7. Protein topology diagram in LDF. (**A**) Conversion of a textbook illustration of a topology diagram into the lithophane format used for testing. From left to right: Digital source image of the topology diagram, front-lit topology diagram lithophane, and back-lit topology diagram lithophane. (**B**) The dimensions of the individual β strands in the lithophane form of the topology diagram are 2.4 cm by 0.45 cm by 0.2 cm. (**C**) Distribution of answers provided by 360 participants for each question regarding the topology diagram lithophane.

can only be approximated. In the case of question #4 of the SDS-PAGE test, the participants were required to approximate the molecular weight of the band in lane 5. The leading edge of this band migrated at ~100 kDa, whereas the lagging edge migrated at ~130 kDa. Because the width of the band spanned ~30 kDa, we accepted a range of answers as being correct (as described in the Supplementary Materials). These correct answers represent a practical gold standard for interpreting how well each cohort visualized the data. We suspect that test participants chose the leading or lagging edge of the band as their reference when selecting their answer. This choice would explain the bimodal distribution of answers for question #4, with the two most common answers being 100 and 130 kDa across different cohorts (Fig. 3).

The average test accuracy for all five lithophanes was 96.7% for blind tactile interpretation, 92.2% for sighted interpretation of back-lit lithophanes, and 79.8% for blindfolded tactile interpretation (Table 1). The accuracy of interpretation of digital imagery on a computer screen was 88.4% by eyesight (Table 1). For ~80% of questions, tactile accuracy by blind chemists was equal or superior to visual interpretation of lithophanes (Table 1). This similarity suggests that lithophanes could function as a shareable data format.

The median and Pearson's second coefficient of skewness (sk_2) were calculated for the 52 datasets that did not have binary answers (Table 1). For 96% of these datasets (50 of 52), the sk_2 value ranged between −2.0 and 2.0 (Table 1). In particular, skewness values were $sk_2 = 0$ for 9 datasets, $sk_2 > 0$ for 27 sets, and $sk_2 < 0$ for 16 sets (Table 1). Only two datasets were highly skewed, with $sk_2 = +2.37$ for the sighted digital cohort answering question #4 of the SDS-PAGE test and $sk_2 = +2.19$ for the blind lithophane cohort answering question #2 of the SEM test (Table 1). The null hypothesis was tested with an unpaired *t* test for sets with $-2 < sk_2 < 2$. For highly skewed datasets ($sk_2 < -2$ or > 2), the null hypothesis was tested using the Kruskal-Wallis *H* test.

We can only speculate why some cohorts achieved higher average scores on some tests compared to other cohorts (or other tests for the same cohort). For example, blindfolded participants performed equally as well as other cohorts in interpreting SEM but scored worse when interpreting SDS-PAGE (Fig. 3 and Table 1). During testing of blindfolded participants on SDS-PAGE, we observed that some participants appeared to inadvertently skip lanes or miscount the lane number on the gel, although the loading wells were still attached. In some cases, it appeared that the test participants thought they were sensing lane 4 but were examining lane 3 or lane 5. Moreover, blind participants interpreted mass spectra with tactile sensing more accurately than the participants of the sighted digital cohort, who were examining an actual digital image of the mass spectra on a computer screen (Fig. 5C and Table 1). We attribute this disparity to the higher educational level of the blind cohort. Four of the five blind persons tested in this study have earned PhDs in the chemical sciences, whereas the sighted participants were undergraduate students enrolled in undergraduate biochemistry, who might have misinterpreted the spectrum.

The ability to accurately interpret lithophanes with tactile sensing is expected considering the millimeter scale of the signal protrusions in printed lithophanes (Figs. 2B, 4B, 5B, 6B, and 7B). The spatial tactile acuity of fingertips has been measured to be 0.94 mm (*21*), and the fingertips can sense nanometer-scale differences in surface roughness (*22*). The tactile sensitivity of blind persons might be greater than sighted persons (by ~0.1 mm); however, these enhancements vary from person to person (*3*). Likewise, the maximum resolution of the human eye is approximately 1 arc min, i.e., ~0.03 mm at a distance of 10 cm (*23*). This scale of tactile graphics in lithophanes, and the distance of visual assessment, can facilitate data sharing where any data that can be seen by eyesight can also be perceived by touch. This universal visualization will likely be moderated, across individuals, by differences in the processing of visual and somatosensory stimuli by the nervous system (*24*). Tactile and visual stimuli are both processed in the visual cortex; however, differences in activity and cross-modal plasticity are observed among early blind, late blind, and sighted individuals (*24*–*28*).

Other methods exist for converting custom 2D imagery into tactile forms (*13*). One common method is swell form technology, also

Table 1. Accuracy of visualization of lithophanes by touch and eyesight.

Data type	Question number*	Blind lithophane†	Sighted lithophane‡	Blindfolded lithophane§	Sighted digital ‖	*P* value
	Accepted answer	*N* = 5	*N* = 106	*N* = 106	*N* = 143	
SDS-PAGE	#1	15.0 ± 0.0	15.8 ± 3.6	19.3 ± 8.6	17.1 ± 5.4	0.0001¶
	15 kDa	(0)	(0.62)	(1.50)	(1.14)	0.0326#
		100%	95.3%	59.4%	77.6%	
	#2	34.0 ± 2.2	34.0 ± 4.3	30.5 ± 9.8	33.5 ± 6.9	0.0009
	30–35 kDa	(−1.34)	(−0.69)	(−1.37)	(−0.64)	0.5116
		100%	91.5%	60.4%	77.6%	
	#3	10.0 ± 0.0	10.8 ± 4.6	17.8 ± 12.8	12.2 ± 8.2	0.0001
	10 kDa	(0)	(0.50)	(1.84)	(0.82)	0.1148
		100%	95.3%	61.3%	79.7%	
	#4	122.0 ± 15.2	104.9 ± 9.4	116.1 ± 13.9	109.1 ± 11.4	0.0001
	100–130 kDa	(−1.57)	(1.56)	(−1.39)	(2.37)	0.0052**
		80%	96.2%	94.3%	99.3%	
	#5	44.0 ± 7.8	50.5 ± 12.9	63.9 ± 31.4	56.0 ± 21.0	0.0001
	47.5 kDa	(−1.34)	(0.71)	(1.57)	(1.21)	0.0179
		80%	84.0%	31.1%	65.0%	
	#6	9.0 ± 0.0	9.0 ± 0.4	8.8 ± 0.9	9.0 ± 0.6	0.0020
	Lane 9	(0)	(0.38)	(−0.70)	(−0.25)	0.1381
		100%	85.9%	48.1%	78.3%	
	Average	93.3%	91.4%	59.1%	79.6%	
Topology	#1	7.00 ± 0.00	7.00 ± 0.00	6.95 ± 0.59	6.90 ± 0.55	0.3919
	7	(0)	(0)	(−0.24)	(−0.54)	0.0876
		100%	100%	95.3%	96.5%	
	#2	↑↓ 5	↑↓ 105	↑↓ 103	↑↓ 143	N/A
	↑↓	100%	99.1%	97.2%	100%	
	Average	100%	99.5%	96.2%	98.3%	
Mass spec	#1	14,500 ± 0	14,521 ± 67	14,514 ± 58	14,516 ± 56	0.4170
	14,500 Da	(0)	(0.94)	(0.70)	(0.85)	0.5225
		100%	80.2%	80.2%	83.2%	
	#2	14,600 ± 0	14,592 ± 27	14,602 ± 37	14,601 ± 39	0.0256
	14,600 Da	(0)	(−0.85)	(0.15)	(0.05)	0.0424
		100%	85.9%	79.3%	83.9%	
	Average	100%	83.0%	79.7%	83.6%	
UV-vis	#1	400.0 ± 0.0	397.6 ± 17.4	393.9 ± 28.0	401.1 ± 25.5	0.2492
	400 nm	(0)	(−0.41)	(−0.65)	(0.12)	0.2243
		100%	96.2%	81.1%	93.0%	
	#2	0.5 ± 0.0	0.50 ± 0.01	0.50 ± 0.05	0.49 ± 0.06	1.0000
	0.50 AU	(0)	(0.41)	(0.18)	(−0.44)	0.3045
		100%	98.1%	88.7%	95.1%	
	Average	100%	97.2%	84.9%	94.1%	

continued on next page

Data type	Question number*	Blind lithophane†	Sighted lithophane‡	Blindfolded lithophane§	Sighted digital ‖	*P* value
	Accepted answer	*N* = 5	*N* = 106	*N* = 106	*N* = 143	
SEM	#1	104.0 ± 16.7	102.1 ± 16.8	103.8 ± 19.7	101.1 ± 22.5	0.4998
	100–120 μm	(0.72)	(0.37)	(0.57)	(0.15)	0.7007
		80%	85.9%	74.5%	83.9%	
	#2	68.0 ± 11.0	63.2 ± 15.6	72.5 ± 20.9	67.6 ± 17.6	0.0003
	40–80 μm	(2.19)	(0.61)	(−1.08)	(1.29)	0.0418
		100%	94.3%	84.0%	88.8%	
	Average	90.0%	90.1%	79.3%	86.4%	
Total		96.7%	92.2%	79.8%	88.4%	

*"Question number" refers to the test question in the Supplementary Materials. "Accepted" answer listed below refers to the value or range of values considered to be correct. †"Blind lithophanes" refers to tactile test of blind subjects. For each cohort, the top value = mean ± SD; middle value = Pearson's second coefficient of skewness (sk_2) in parentheses; bottom value = accuracy listed as %. ‡ "Sighted lithophane" refers to sighted participants who used eyesight to interpret lithophanes. § "Blindfolded lithophane" refers to tactile test of blindfolded participants (who were sighted). ‖ "Sighted digital" refers to sighted participants who used eyesight to interpret master digital image. ¶*P* value compares average answer (top value) between sighted lithophane and blindfolded lithophane groups. An unpaired *t* test was used. #*P* value compares average answer (top value) between sighted lithophane and sighted digital groups. An unpaired *t* test was used. **P value compares whether samples originate from the same distribution between sighted lithophane and sighted digital groups. A Kruskal-Wallis *H* test was used for this skewed dataset, instead of an unpaired *t* test.

known as "pictures in a flash" technology (*13*). Here, specialized paper ("swell form paper") is used to make soft, foam-like tactile graphics. When heated, micrometer-size alcohol granules in the paper induce swelling in regions that have been printed with black ink or toner (color ink is not raised). The primary advantage of swell form, over the lithophane format, is that it is faster than 3D printing. The primary disadvantage is that swell form technology cannot controllably produce tactile graphics at the same accuracy, resolution, and variable height that is possible with current 3D printing.

To illustrate some of these points, we made tactile graphics using swell form technology (fig. S3). Graphics were made from the same digital images used to make lithophanes. Several regions of the printed image remained flat during heating (fig. S3, C to E), despite being printed clearly by the laser printer (and despite a maximum setting of "10" on the ZY Form machine).

Printed regions that failed to swell included bands in the SDS-PAGE (fig. S3, B and C), chitin fibrils (fig. S3D), and loops in the topology diagram (fig. S3E). Other regions deformed or swelled into neighboring signals (fig. S3, B to D). For example, some bands in the SDS-PAGE were distorted to craters or pancakes and did not project as 3D peaks (fig. S3, B and C). Other bands swelled into each other (fig. S3, B and C). Although most chitin fibrils did not swell—despite being printed—others swelled into each other, resulting in loss of fibril resolution (fig. S3D). The mass spectrum was accurately depicted except for spectral noise (fig. S3F): Tactile graphics were raised outside the printed ink (fig. S3F). Swell form technology did work well for the UV-vis dataset (fig. S3G).

Although this study did not examine chromatic data, we expect that the visualization of colored data—for example, heatmaps and 2D color plots—can be accomplished with lithophanes projecting a monotonic grayscale. To be useful in quantitative data interpretation, the digital image will need to be converted into a color space such as "cube helix" that is designed to convert to a monotonic grayscale of gradually increasing brightness (*29*). The more common color spaces such as HSV (hue, saturation, value), which do not result in a monotonic grayscale, would not be ideal because different colors would have identical thickness (brightness) in the lithophane (e.g., cyan and yellow are equivalent in the grayscale of HSV).

Data for all

People with blindness have been historically discouraged from learning chemistry and have been kept out of the laboratory (*30*, *31*). The irony of this ableism is nanoscale. Atoms and molecules are smaller than 250 nm, which happens to be the diffraction limit of visible light. This mismatch is why we are all blind to molecules (*30*). It is partly why an "atom in a molecule" has been described as a Kantian noumenon, unknowable by observation but conceivable by reason (*32*). To try and see something about them, we must use spectroscopy, microscopy, or painstakingly grow crystals that diffract x-rays (or neutrons or electrons). Even then, we must build ourselves artificial eyes to detect how photons, neutrons, or electrons interact with atoms and molecules.

Then, after lastly getting a peek at the atomic world, scientists eagerly make graphical diagrams to show us what they saw: G. Lewis and his dot structures (*33*), J. Richardson's ribbon diagrams (*34*), and C. Levinthal's computer graphics (*35*). Taking one final step to make this imagery accessible to all people is now easier than ever. The types of lithophanes described here can be produced by any science department at any university, or in any high school science laboratory or classroom. The lithophane data format (LDF) is by no means limited to pictures in science. Lithophanes can be used in the inclusive design (*36*) of imagery throughout the fine arts, economics, humanities, business, government, health sciences, and law (*37*–*45*).

MATERIALS AND METHODS

Fabrication of lithophane forms of common data

SDS-PAGE dataset

SDS-PAGE experiments were performed using standard protocols. Briefly, SDS-PAGE was performed using commercial gels (Invitrogen

NuPAGE 12% bis-tris 1.0 mini protein gels; 10 wells). To calibrate band migration with molecular weight, a prestained molecular weight marker or "protein ladder" was loaded into lane 1 (PageRuler Plus; Thermo Fisher Scientific; catalog no. 26619; see Fig. 2A). Proteins were purchased from Sigma-Aldrich and loaded into lanes 2 to 10 in the following order: cytochrome c (lane 2), carbonic anhydrase (lane 3), ubiquitin (lane 4), phosphorylase b (lane 5), and ovalbumin (lane 6). Lanes 7 to 10 were loaded with mixtures of these proteins. Electrophoresis was performed for 45 min at 200 V. After staining with Coomassie brilliant blue, the gel was destained overnight before imaging with a Bio-Rad Gel Doc EZ imager. The resulting image was saved as a portable network graphic (.PNG) file. This image of the gel (shown in Fig. 2) was used to create the lithophane form of the exact image (without any digital alteration of the image).

Another SDS-PAGE experiment was performed (using the same methods) to quantify the correlation between signal intensity from a digital image of the back-lit lithophane (of the gel) and the signal intensity of the raw digital image of the actual gel. This second experiment was used not to create materials for testing on participants but only to determine the signal correlation between digital images of the gel and back-lit lithophane. This gel was loaded with a dilution series of both carbonic anhydrase (purchased from Thermo Fisher Scientific) and recombinant human wild-type SOD1 purified from *Saccharomyces cerevisiae*. The signal intensity of bands in the dilution series was analyzed with (i) densitometry of the digital image of the polyacrylamide gel (using ImageJ) and (ii) identical densitometry of a digital image of the back-lit lithophane of the gel. Signal intensities of each band from the lithophane and gel were plotted against each other.

Electrospray ionization mass spectrometry dataset

A mass spectrum of a protein was acquired using a Thermo Orbitrap Discovery mass spectrometer. The mass spectrum that was collected was of human α-synuclein, with two gas phase phosphate adducts (+98 Da). This is the only mass spectrum collected and the one used for testing. The α-synuclein protein was recombinantly expressed in *Escherichia coli*. For MS analysis, the protein sample (150 mM) was diluted 100-fold into a mixture of 69.95% acetonitrile, 29.95% water, and 0.1% formic acid. The mass spectrum was deconvoluted using the MaxEnt 1 module in MassLynx software. The deconvoluted *x*/*y* coordinates of this spectrum were exported and converted to a .PNG file for printing into the lithophane format.

Electronic (UV-vis) spectroscopy dataset

A UV-vis electronic spectrum of horseradish peroxidase was acquired using a Shimadzu UV 2550 spectrophotometer. Absorbance was measured from 300 to 600 nm and intensity values ranged from 0.0 to 0.6 absorbance units. Coordinates (*x*/*y*) of this spectrum were exported from the spectrophotometer.

Protein topology dataset

The topology diagram of the antiparallel seven β strand protein was created using Adobe Illustrator.

SEM dataset

The SEM lithophane of a single butterfly scale was acquired using a Versa 3D SEM (FEI, OR, USA). The pieces of butterfly wing (Gulf Fritillary, *Agraulis* sp.) that were imaged were harvested during a previously published study (*46*). Samples were air-dried and then mounted on aluminum stubs with carbon tape.

Fabrication of lithophanes from digital images of datasets

Each lithophane layout was printed using PreForm software and a formlabs 3B+ stereolithographer. .PNG files were converted to STereoLithography (.STL) files using an image to lithophane generator (3dp.rocks/lithophane/). Model parameters for each lithophane consisted of a maximum size of 100 mm, a maximum thickness of 2.5 mm, a thinnest layer of 0.5 mm, and four vectors per pixel. All other settings were kept at a value of 0. For SEM, the contrast of images was inverted. Here, the butterfly wing SEM was transformed into the negative contrast image (dark shades inverted to light shades; light converted to dark) to produce a lithophane where the previously dark areas in the raw data are now brightest (thinnest) and the lighter areas in the original image are now darkest and thickest (see inset, Fig. 4).

Models were then constructed using gray photopolymer resin (composed of urethane dimethylacrylate, methacrylate monomer, and photoinitiator). Each lithophane was printed at a resolution of 100 μm with necessary supports. After printing, lithophanes were washed in an enclosed, circulating bath (Form Wash, Formlabs) containing food-grade isopropyl alcohol for 10 min. Lithophanes were then cured with UV light using a Form Cure at 60°C for 30 min. The supports were then removed with a gloved hand.

Fabrication of swell form graphics

The exact same digital images used to create lithophanes were also printed onto swell form paper (Zytex2 Swell Paper). Printing was accomplished using a laser printer to produce images that were identical in size and shade to those used to produce lithophanes. The laser printer (Hewlett Packard Color LaserJet Enterprise M653) was operating on default settings. These printed sheets were fed through a thermal swell form machine (a ZY-Fuse machine) on a setting of 7 to 10 to produce tactile graphics.

Study participants and assessment

This study has been approved by the Institutional Review Board at Baylor University. Tests were performed on 360 persons, broken down into two general cohorts and additional subcohorts. The first test cohort consisted of 355 undergraduate students who were enrolled in an introductory biochemistry course at the time of testing (at Baylor University). Of these 355 college students who participated, ~67% were identified as female and ~33% were identified as male. This distribution is consistent with the enrollment demographics of this class at Baylor University. The visual acuity (corrected) of the 355 students was in the range of normal, with 77% of students having a corrected vision of 20/20 or better. The second cohort in the study involved five persons with blindness who have experienced total blindness or low vision since childhood or adolescence. Four of these persons have earned PhD degrees in chemistry before testing, and the fifth person is an undergraduate student at Baylor University who experienced complete vision loss during their senior year in high school.

Of the first cohort of 355 students, 212 students were asked to examine each of the five lithophanes (Figs. 2 to 7) by either eyesight (n = 106) or manual tactile sensing while blindfolded (n = 106). Of the 212 students who examined lithophanes, 106 (50%) of the students were asked to use tactile sensing (fingers and hands) to interpret lithophanes. Here, students were provided with a blindfold and a lithophane. The other 106 students were given only lithophanes and were asked to interpret them with eyesight and backlighting. Here, students were instructed to hold their lithophanes up to the ceiling lights in the classroom (Sylvania Octron Supersaver 28-W fluorescent bulbs). The classroom was a lecture hall with ~15-foot-high ceilings. These students were instructed to not use tactile sensing. All of these

students were present in a standard size classroom on the campus of Baylor University, with researchers present during testing. The remaining 143 students were asked to use eyesight to interpret the digital master images of data from which the lithophanes were made. No students were excluded from this study on the basis of any criteria, and the assignment of testing by tactile sense or eyesight was arbitrary.

Of the 106 students who participated in tactile testing of lithophanes, each was given a blindfold (sleeping mask) and a box containing five separate nontransparent (black) Ziploc bags in which were five different lithophanes (those shown in Figs. 2 and 4 to 7). Bags were labeled according to the lithophane they contained (SDS-PAGE, Topology, Mass spec, UV-vis, and SEM). The label also contained a QR code that directed students to a URL on their phone, where students could enter answers to questions for each test. For the SDS-PAGE lithophane, the participants were asked to answer each of the following six questions. Question #1: What is the mass (in kilodaltons) of the protein in lane 2? Question #2: What is the mass (in kilodaltons) of the protein in lane 3? Question #3: What is the mass (in kilodaltons) of the protein in lane 4? Question #4: What is the mass (in kilodaltons) of the major protein in lane 5? Question #5: What is the mass (in kilodaltons) of the two proteins in lane 6? Question #6: Which lane between 7 and 10 is the purest (least number of bands)?

For the topology lithophane, the participants were asked to answer two questions. Question #1: How many β strands (arrows) are there? Question #2: Are the arrows parallel or antiparallel?

For the MS lithophane, the participants were also given two questions. Question #1: What is the mass of the most intense peak? Question #2: What is the mass of the second most intense peak?

For the UV-vis lithophane, two questions were asked. Question #1: What is the wavelength (x axis) in nanometers of the highest peak? Question #2: What is the absorbance (y axis) in absorbance units of the highest peak?

For the SEM lithophane, two questions were asked. Question #1: What is the length (horizontal) in micrometers of the single butterfly scale? Question #2: What is the width (vertical) in micrometers of the single scale on the butterfly wing? The answers for each test question are provided in the Supplementary Materials (data S1).

Students were not given a set amount of time for each test. However, tests did not exceed 15 min for any given lithophane. Blindfolded students wore their blindfolds during all testing and were only removed (after putting the lithophane back into the Ziploc bag) to enter answers into their phone. Because most blind persons do not read Braille, we used a computerized voice to read aloud pertinent axis information required to answer each question (using the text-to-audio function in Microsoft Word).

The 143 participants who were asked to interpret digital images with eyesight were provided the electronic .PNG image used to create each lithophane (using internet-based web conferencing such as Zoom) and were tested with the same instructions as described above. For all 355 students, a brief refresher of the analytical techniques used to collect data was provided before testing (e.g., to ensure students could interpret molecular weight ladders and electrophoresis of proteins in a gel matrix). Furthermore, a short review of topology was given so that students could interpret parallel versus antiparallel β strands.

For the second cohort of persons with blindness, the same boxes and lithophanes as described above for students who tested in-person were delivered to blind persons before testing. The packaging remained sealed until the start of the test. Rather than having the blind or visually impaired chemist scan the QR code and manually submit their answers, answers were recorded by the test proctor. Each question was read aloud to participants followed by answer choices. These choices were repeated to the individual at their request until an answer was given. Each test was not allowed to exceed 15 min. A refresher was given on the interpretation of SDS-PAGE and protein topology diagrams. The same computerized voice in Word was used during each test.

Each question in each test was designed to have only one correct response. However, a few questions had room for interpretation due to the nature of the data. Regarding the SDS-PAGE, particularly questions #2 and #4, the major protein band had a thickness that spanned a wide range of molecular weight values due to the nonlinear nature of SDS-PAGE. For question #2, two values were provided that were accepted as correct (30 and 35 kDa). For question #4, several values were provided that were accepted as correct (100 to 130 kDa). The nonuniform shape of the single butterfly scale left the length and width to be up for interpretation. For the length, a value of 100 to 120 μm was accepted, and for the width, a value of 40 to 80 μm was accepted as a correct answer.

Statistical analysis

Statistical analysis was used to quantify test accuracy for all cohorts, to test the skewness of data, and to test the null hypothesis between datasets of certain cohorts. For each cohort, given answers were expressed as a mean with SD. The median and Pearson's second coefficient of skewness (sk_2) were calculated for all datasets (excluding questions with binary answers, e.g., parallel or antiparallel β strands). For datasets with $sk_2 > -2$ or < 2, an unpaired t test was used to calculate P values related to mean answers provided by the sighted lithophane cohort and blindfolded cohort, as well as between the sighted lithophane cohort and the sighted digital cohort (Table 1). For highly skewed data ($sk_2 < -2$ or >2), a Kruskal-Wallis H test was used to calculate P values in lieu of an unpaired t test.

SUPPLEMENTARY MATERIALS

Supplementary material for this article is available at https://science.org/doi/10.1126/sciadv.abq2640

View/request a protocol for this paper from *Bio-protocol*.

REFERENCES AND NOTES

1. E. Brown, Disability awareness: The fight for accessibility. *Nature* **532**, 137–139 (2016).
2. Y. H. Wu, N. Martiniello, B. K. Swenor, Building a more accessible conference for researchers with vision impairment. *JAMA Ophthalmol.* **140**, 113–114 (2022).
3. K. M. Baumer, J. J. Lopez, S. V. Naidu, S. Rajendran, M. A. Iglesias, K. M. Carleton, C. J. Eisenmann, L. R. Carter, B. M. Shaw, Visualizing 3D imagery by mouth using candy-like models. *Sci. Adv.* **7**, eabh0691 (2021).
4. A. Kizilaslan, S. L. Zorluoglu, M. Sozbilir, Improve learning with hands-on classroom activities: science instruction for students with visual impairments. *Eur. J. Spec. Needs. Edu.* **36**, 371–392 (2020).
5. J. J. Yerbury, R. M. Yerbury, Disabled in academia: To be or not to be, that is the question. *Trends Neurosci.* **44**, 507–509 (2021).
6. J. P. Sarju, Nothing about us without us - towards genuine inclusion of disabled scientists and science students post pandemic. *Chem. A Eur. J.* **27**, 10489–10494 (2021).
7. I. S. Daehn, P. L. Croxson, Disability innovation strengthens STEM. *Science* **373**, 1097–1099 (2021).
8. K. Powell, M. Minkara, Chemical modelling with a sense of touch. *Nature* **595**, 756–756 (2021).
9. B. Swenor, L. M. Meeks, Disability inclusion—Moving beyond mission statements. *N. Engl. J. Med.* **380**, 2089–2091 (2019).
10. R. J. Peterson, We need to address ableism in science. *Mol. Biol. Cell* **32**, 507–510 (2021).

11. C. A. Supalo, S. H. Kennedy, Using commercially available techniques to make organic chemistry representations tactile and more accessible to students with blindness or low vision. *J. Chem. Educ.* **91**, 1745–1747 (2014).
12. H. B. Wedler, S. R. Cohen, R. L. Davis, J. G. Harrison, M. R. Siebert, D. Willenbring, C. S. Hamann, J. T. Shaw, D. J. Tantillo, Applied computational chemistry for the blind and visually impaired. *J. Chem. Educ.* **89**, 1400–1404 (2012).
13. M. Mukhiddinov, S. Y. Kim, A systematic literature review on the automatic creation of tactile graphics for the blind and visually impaired. *Processes* **9**, 1726 (2021).
14. M. Carney, Lithophanes … not a dead art form. *Ceramics: Art and Perception* **87**, 24–29 (2012).
15. M. Carney, *Lithophanes* (Schiffer Publishing Ltd., 2008), 224 pp.
16. S. H. H. Han, J. Ko, Parameter study of lithophane for efficient reproduction of 2D image as 3D object using 3D printing. *J. Korean Soc. Mar. Eng.* **43**, 793–797 (2019).
17. G. A. Fernandez, R. A. Ocampo, A. R. Costantino, N. S. Dop, Application of didactic strategies as multisensory teaching tools in organic chemistry practices for students with visual disabilities. *J. Chem. Educ.* **96**, 691–696 (2019).
18. J. R. Miecznikowski, M. J. Guberman-Pfeffer, E. E. Butrick, J. A. Colangelo, C. E. Donaruma, Adapting advanced inorganic chemistry lecture and laboratory instruction for a legally blind student. *J. Chem. Educ.* **92**, 1344–1352 (2015).
19. A. V. Huynh, P. Stein, E. D. Buhr, 3D-printed assistive pipetting system for gel electrophoresis for technicians with low acuity vision. *Biotechniques* **70**, 49–53 (2021).
20. "The Braille Literacy Crisis in America," *A Report to the Nation by the National Federation of the Blind* (The Jernigan Institute, 2009).
21. R. W. Van Boven, K. O. Johnson, The limit of tactile spatial resolution in humans: Grating orientation discrimination at the lip, tongue, and finger. *Neurology* **44**, 2361–2366 (1994).
22. B. L. Miles, K. Van Simaeys, M. Whitecotton, C. T. Simons, Comparative tactile sensitivity of the fingertip and apical tongue using complex and pure tactile tasks. *Physiol. Behav.* **194**, 515–521 (2018).
23. H. P. Bowditch, W. F. Southard, A comparison of sight and touch. *J. Physiol.* **3**, 232–245 (1882).
24. K. Sathian, Visual cortical activity during tactile perception in the sighted and the visually deprived. *Dev. Psychobiol.* **46**, 279–286 (2005).
25. A. Ankeeta, S. Senthil Kumaran, R. Saxena, S. N. Dwivedi, N. R. Jagannathan, Visual cortex alterations in early and late blind subjects during tactile perception. *Perception* **50**, 249–265 (2021).
26. K. Sathian, A. Zangaladze, Feeling with the mind's eye: Contribution of visual cortex to tactile perception. *Behav. Brain Res.* **135**, 127–132 (2002).
27. A. Zangaladze, C. M. Epstein, S. T. Grafton, K. Sathian, Involvement of visual cortex in tactile discrimination of orientation. *Nature* **401**, 587–590 (1999).
28. L. A. Renier, I. Anurova, A. G. De Volder, S. Carlson, J. VanMeter, J. P. Rauschecker, Preserved functional specialization for spatial processing in the middle occipital gyrus of the early blind. *Neuron* **68**, 138–148 (2010).
29. D. A. Green, A colour scheme for the display of astronomical intensity images. *Bull. Astron. Soc. India* **39**, 289–295 (2011).
30. H. B. Wedler, R. L. Davis, D. Flynn, A. Franz, C. S. Hamann, J. G. Harrison, M. W. Lodewyk, K. A. Milinkevich, J. T. Shaw, D. J. Tantillo, S. C. Wang, Nobody can see atoms: Science camps highlighting approaches for making chemistry accessible to blind and visually impaired students. *J. Chem. Educ.* **91**, 188–194 (2014).
31. G. M. Nepomuceno, D. M. Decker, J. D. Shaw, L. Boyes, D. J. Tantillo, H. B. Wedler, The value of safety and practicality: Recommendations for training disabled students in the sciences with a focus on blind and visually impaired students in chemistry laboratories. *J. Chem. Health Saf.* **23**, 5–11 (2016).
32. R. G. Parr, P. W. Ayers, R. F. Nalewajski, What is an atom in a molecule? *J. Phys. Chem. A* **109**, 3957–3959 (2005).
33. G. N. Lewis, The atom and the molecule. *J. Am. Chem. Soc.* **38**, 762–785 (1916).
34. J. S. Richardson, D. C. Richardson, D. S. Goodsell, Seeing the PDB. *J. Biol. Chem.* **296**, 100742 (2021).
35. L. Katz, C. Levinthal, Interactive computer graphics and representation of complex biological structures. *Annu. Rev. Biophys. Bioeng.* **1**, 465–504 (1972).
36. T. Lloyd-Esenkaya, V. Lloyd-Esenkaya, E. O'Neill, M. J. Proulx, Multisensory inclusive design with sensory substitution. *Cogn. Res. Princ. Implic.* **5**, 37 (2020).
37. S. Singh, A. M. Khan, U. Dhaliwal, N. Singh, Using the health humanities to impart disability competencies to undergraduate medical students. *Disabil. Health J.* **15**, 101218 (2022).
38. A. Correa, M. H. Masuchi, N. Baeta, L. Takiuchi, B. Bianco, Disability inclusion in higher education: Knowledge and perceptions of the academic community. *Disabil. Rehabil. Assist. Technol.* **16**, 735–740 (2021).
39. M. Lyner-Cleophas, Assistive technology enables inclusion in higher education: The role of higher and further education disability services association. *Afr. J. Disabil.* **8**, 558 (2019).
40. L. Wang, Perspectives of students with special needs on inclusion in general physical education: A social-relational model of disability. *Adapt. Phys. Activ. Q.* **36**, 242–263 (2019).
41. E. Carthy, Being positive on disability in medical education. *BJPsych Bull.* **45**, 193–194 (2021).
42. K. Mulligan, A. Calder, H. Mulligan, Inclusive design in architectural practice: Experiential learning of disability in architectural education. *Disabil. Health J.* **11**, 237–242 (2018).
43. M. Sabatello, B. J. Insel, T. Corbeil, B. G. Link, P. S. Appelbaum, The double helix at school: Behavioral genetics, disability, and precision education. *Soc. Sci. Med.* **278**, 113924 (2021).
44. K. Viscardis, C. Rice, V. Pileggi, A. Underhill, E. Chandler, N. Changfoot, P. Montgomery, R. Mykitiuk, Difference within and without: Health care providers' engagement with disability arts. *Qual. Health Res.* **29**, 1287–1298 (2019).
45. P. Blanck, Disability inclusive employment and the accommodation principle: Emerging issues in research, policy, and law. *J. Occup. Rehabil.* **30**, 505–510 (2020).
46. B. Zechmann, Beam deceleration improves Image quality of butterfly wing scales in the scanning electron microscope. *Texas J. Microsc.* **49**, 26–27 (2018).

Acknowledgments: We would like to thank D. Jonklaas and M. Lahousse for assistance during the testing of lithophanes in classroom settings at Baylor University. We would also like to thank L. Hospital, A. Wolf, S. Merritt, S. O'Brien, and J. Allan at the Texas School for the Blind and Visually Impaired for helpful discussions. **Funding:** This work was funded by National Science Foundation grant 1856449 (to B.F.S.), Welch Foundation grant AA-1854 (to B.F.S.), and NIH grant R25GM146265 (to B.F.S.). **Author contributions:** Conceptualization: B.F.S., J.C.K., and C.M.D. Methodology: J.C.K., C.M.D., E.A.A., J.J.L., M.A.I., B.Z., and B.F.S. Data curation: J.C.K., C.M.D., K.-S.P., B.Z., and B.F.S. Investigation: B.F.S., J.C.K., C.M.D., J.J.L., and M.A.I. Visualization: B.F.S., J.C.K., C.M.D., J.J.L., M.A.I., and B.Z. Writing—original draft: B.F.S., J.C.K., and C.M.D. Writing—review and editing: All authors. **Competing interests:** C.A.S. is employed at a company that develops and sells assistive technology to people with blindness. All other authors declare that they have no competing interests. **Data and materials availability:** All data needed to evaluate the conclusions in the paper are present in the paper and/or the Supplementary Materials.

Submitted 28 March 2022
Accepted 17 June 2022
Published 17 August 2022
10.1126/sciadv.abq2640

ScienceAdvances

Data for all: Tactile graphics that light up with picture-perfect resolution

Jordan C. KooneChad M. DashnawEmily A. AlonzoMiguel A. IglesiasKelly-Shaye PateroJuan J. LopezAo Yun ZhangBernd ZechmannNoah E. CookMona S. MinkaraCary A. SupaloHoby B. WedlerMatthew J. Guberman-PfefferBryan F. Shaw

Sci. Adv., 8 (33), eabq2640. • DOI: 10.1126/sciadv.abq2640

Science Advances (ISSN) is published by the American Association for the Advancement of Science. 1200 New York Avenue NW, Washington, DC 20005. The title *Science Advances* is a registered trademark of AAAS.